Cellular Physiology and Biochemistry

Cell Physiol Biochem 2020;54:71-87
DOI: 10.33594/000000206
Published online: 24 January 2020
Accepted: 29 December 2019

Original Paper

Integrin Linked Kinase (ILK) Downregulation as an Early Event During the Development of Metabolic Alterations in a Short-Term High Fat Diet Mice Model

Marco Hatem-Vaquero[a,b] Mercedes Griera[a,b] Diego Garcia-Ayuso[a,b] Sofia Campillo[a,b] Lourdes Bohorquez[a,b] Laura Calleros[a,b] Diego Rodriguez-Puyol[b,c] Manuel Rodriguez-Puyol[a,b] Sergio de Frutos[a,b]

[a]Department of Systems Biology, Physiology Unit, from Universidad de Alcalá, Alcalá de Henares, Madrid, Spain, [b]Instituto Ramón y Cajal de Investigación Sanitária (IRYCIS), Fundación Renal Iñigo Álvarez de Toledo (FRIAT) and REDinREN from Instituto de Salud Carlos III, Madrid, Spain, [c]Biomedical Research Foundation and Nephrology Unit from Hospital Príncipe de Asturias and Department of Medicine from Universidad de Alcalá, Alcalá de Henares, Madrid, Spain

Key Words
Integrin linked kinase • Insulin resistance • Inflammation • Lipolysis • Gluconeogenesis

Abstract
Background/Aims: Diabetes type 2, metabolic syndrome or non-alcoholic fatty liver disease are insulin resistance-related metabolic disorders, which lack a better prognosis before their full establishment. We studied the importance of the intracellular scaffold protein integrin linked kinaes (ILK) as a key modulator in the initial pathogenesis and the early progression of those insulin resistance- related disorders. ***Methods:*** Adult mice with a global transgenic downregulation of ILK expression (cKD-ILK) and littermates without that depletion (CT) were fed with either standard (STD) or high fat (HFD) diets during 2 and 6 weeks. Weights, blood glucose and other systemic biochemical parameters were determined in animals under fasting conditions and after glucose or pyruvate intraperitoneal injections to test their tolerance. In RNA or proteins extracted from insulin-sensitive tissues, we determined by reverse transcription–quantitative PCR and western blot the expression of ILK, metabolites transporters and other metabolism and inflammatory markers. Glucose uptake capacity was studied in freshly isolated tissues. ***Results:*** HFD feeding was able to early and progressively increase glycaemia, insulinemia, circulating glycerol, body weight gain, liver-mediated gluconeogenesis along this time lapse, but cKD-ILK have all these systemic misbalances exacerbated compared to CT in the same HFD time lapse. Interestingly, the tisular expression of ILK in HFD-fed CT was dramatically downregulated in white adipose tissue (WAT), skeletal muscle and liver at the

S. de Frutos, D. Rodríguez-Puyol and M. Rodríguez-Puyol contributed equally to this work.

Sergio de Frutos, Ph.D. Dpt. de Biología de Sistemas, Unidad Fisiología, A2 KM 33,600, Campus Universidad de Alcalá Facultad de Medicina, Universidad de Alcalá, Alcalá de Henares, Madrid, 28805 (Spain)
Tel. 34918854519, Fax 34918854590, E-Mail sergio.frutos@uah.es

same extent of the original ILK downregulation of cKD-ILK. We previously published that basal STD-fed cKD-ILK compared to basal STD-CT have different expression of glucose transporters GLUT4 in WAT and skeletal muscle. In the same STD-fed cKD-ILK, we observed here the increased expressions of hepatic GLUT2 and WAT pro-inflammatory cytokines TNF-α and MCP-1. The administration of HFD exacerbated the expression changes in cKD-ILK of these and other markers related to the imbalanced metabolism observed, such as WAT lipolysis (HSL), hepatic gluconeogenesis (PCK-1) and glycerol transport (AQP9). ***Conclusion:*** ILK expression may be taken as a predictive determinant of metabolic disorders establishment, because its downregulation seems to correlate with the early imbalance of glucose and glycerol transport and the subsequent loss of systemic homeostasis of these metabolites.

Introduction

Chronic metabolic disorders connected to insulin resistance, such as diabetes type 2, non-alcoholic fatty liver disease or the group defined as metabolic syndrome have a multifactorial etiology and implicates the inter-communication between metabolically relevant tissues, which complicates the quest of the pathogenesis. Some of the characteristic events that may occur during their progression are: 1) hyperglycemia together with the defective transport and disposal of glucose in the tissues [1], 2) the increase of lipolysis events within the white adipose tissue (WAT) [2] and 3) the increase of gluconeogenesis in the liver [3, 4].

Erratic expression of transmembrane transporters such as glucose transporters GLUT4 in muscle and WAT, GLUT2 in the liver or hepatic glycerol channel aquaporin AQP9 [5-7] are implicated during the dysfunctional cellular uptake from blood stream of glucose and lipolysis sub-products. Pancreatic β-cell expansion also correlates with global and complex metabolites changes on rodent models in response to high fat diet (HFD) [8]. Moreover, WAT increases the secretion of several pro-inflammatory adipokines such as tumor necrosis factor α (TNFα) and monocyte chemoattractant protein-1 (MCP-1), which allow a general low-grade inflammatory state in WAT and other organs [2]. In turn, the increased circulating pro-inflammatory adipokines and metabolic products will persevere the unbalanced processing of metabolites.

In the search for the origin of insulin sensitivity loss, others and we suggested that integrin-linked kinase (ILK) might be a potential modulator of insulin sensitivity decrease [9-11]. ILK is an intracellular scaffold protein which is able to mediate between the extracellular environment and the cell, and according to our previous research it may be assigned as a basal transcriptional and/or post-transduction modulator of transmembrane transporters such as GLUT4 or AQP2 [9, 12, 13]. Here we further elucidate the implication of ILK in the pathogenesis of insulin resistance during the early establishment of a HFD-fed mice model [15-17]. We challenged transgenic mice with global ILK downregulated expression in their adulthood (cKD-ILK) [9] and their control counterparts (CT, with the same transgenic background but without ILK depletion induced) with either HFD or the corresponding low fat standard diet (STD) for a short-term period of 2 and 6 weeks. During this HFD-based early stage, the expression of ILK in insulin sensitive tissues relates with the early unbalance in glucose and glycerol transport, pro-inflammation, lipolysis, gluconeogenesis and subsequent body weight gain and systemic glucose and insulin loss of homeostasis.

Materials and Methods

Animal model and diets

All procedures involving animals were approved by the Institutional Animal Care Committees of the University of Alcalá and Comunidad de Madrid, in agreement with the guidelines established by the European Community Council Directives (2010/63/EU). Adult conditional ILK-deficient mice (cKD-ILK) were generated as previously described [9]. Briefly, C57Bl/6 mice homozygous for floxed ILK flanked by

loxP (LOX) were crossed with BALB/c strain mice carrying a CMV-driven hydroxytamoxifen -inducible (TX, Sigma-Aldrich, St. Louis, MO, USA) CreER (T) recombinase gene (CRE) globally expressed in all the tissues. Male CRE-LOX (8-week-old) were injected intraperitoneal with 1.5 mg of TX or vehicle (VH), once per day for 5 consecutive days. 3 weeks after the injections, tail DNA was genotyped by PCR with primers corresponding to excised ILK gene (CCAGGTGGCAGAGGTAAGTA) or to non-excised ILK (CAAGGAATAAGGTGAGCTTCAGAA). The TX-treated CRE-LOX mice displaying successful depletion of ILK were termed cKD-ILK, and the VH-treated CRE-LOX without ILK depletion were termed control (CT). At that point, mice were fed for a total of 2 and 6 weeks either with a High Fat diet (HFD, 60 kJ% fat, 8.46 % sucrose; D12492 Ssniff Spezialdiäten, Soest, Germany) or the corresponding low fat standard diet (STD, 13 kJ% fat, 67Kj% carbohydrates, 10 % sucrose; Envigo Teklad Global Diet 2014, East Millstone, NJ, USA). The food intakes were calculated by subtracting the mass of food left from the initial food supplied, and expressed as mean per day along every week. None differences of grams ingested per diet between weeks were observed through the whole period of the diet challenges. Table 1 detail diets composition and animal intakes. Age-matched males and females mice were divided randomly into different groups: fed with HFD or standard diet for 2 and 6 weeks. Diets were given ad libitum during the time of the experiment. Each mouse had free access to water and was kept on a 12:12 h light:dark cycle at constant temperature of 21–23 °C. N per group and experiment was between 6 and 12, detailed in the figure legends and/or results section. Prior to any determination, mice were maintained under fasting conditions for 16 h. Animals were weighted and euthanized with pentobarbital overdose after the experimentations conclude. Body weight gains were calculated subtracting weights at the beginning from weights at the end of each experimental timeline. Epididymal WAT depots, slow-twitch red fibers from the vastus lateralis muscle and the right medial lobe of liver were dissected and freshly processed or after preservation in RNAlater (Thermo Fisher Scientific, Waltham, MA, USA).

Table 1. Diets composition and food (g) and caloric (Kcal) intakes per 24 h, represented as means ± SEMs from a total of n=6 animals per group; *= P<0.05 vs STD

DIET COMPOSITION	Low fat /low sugar Diet (STD)		High fat /low sugar Diet (HFD)	
Commercial Company	Global Diet 2014, Envigo Teklad, East Millstone, NJ, USA		D12492, Ssniff Spezialdiäten, Soest, Germany	
Fat (%)	4.0		34.6	
Carbohydrates (%)	48.0		20.0	
Proteins (%)	14.3		24.0	
Sucrose (%)	10.0		8.5	
METABOLIZABLE ENERGY (Kcal/g)	3		6	
Calories from Fat (%)	13		60	
Calories from Carbohydrates (%)	67		20	
Calories from Protein (%)	20		20	
Fat source	Soy oil		31.5% pork lard + 3.1 % soy oil	
Saturated fatty acids (%)	0.6		13.5	
Monounsaturated fatty acids (%)	0.7		14.9	
Polyunsaturated fatty acids (%)	2.1		34.0	
Mineral and traces (%)	6.0		6.0	
FOOD INTAKE	(g/24 h)	(Kcal/24h)	(g/24 h)	(Kcal/24h)
CT	3.45± 0.33	9.97± 0.96	2.37 ± 0.09*	14.13± 0.53*
cKD-ILK	3.57± 0.34	10.33± 0.97	2.37± 0.07*	14.51± 0.41*

Analysis of biochemical parameters

In vivo blood parameters determinations were taken along the time via tail bleeding in a group of cKD-ILK and CT fed with HFD during 6 weeks at the following time points: 0, 2 and 6 weeks of HFD. Fasting glucose was determined using a glucometer (Accu-Check Aviva; Roche, Basel, Switzerland). Heparinized blood samples were centrifuged (900 g, 15 min, 4ºC) and commercial kits were used to determine in plasma insulin (Cloud-Clone Corp., Houston, TX, USA), free glycerol, free fatty acid, Plasma triglycerides, total cholesterol and HDL (Biovision, Milpitas, CA, USA). The homeostasis model assessment of insulin resistance (HOMA-IR) in the animals were calculated according to the formula fasting glucose (mg/dl) × fasting insulin (mU/L)/405.

Glucose and pyruvate tolerance tests (GTT and PTT)

cKD-ILK and CT fed with HFD during 6 weeks were devoted to perform tolerance tests along the same time points: 0, 2 and 6 weeks of HFD. The mice fasting for16 h were i.p. injected with glucose or sodium pyruvate (2 mg per g of body weight, Sigma-Aldrich, St. Louis, MO, USA) and blood glucose levels were measured at times 0, 30, 90, 150 and 180 min after bolus. Total areas under the curve (AUC) obtained during GTT and PTT were calculated [9, 18].

Glucose uptake assay

Glucose uptake capacity of freshly excised tissues was performed as described previously [9]. Briefly, excised epididymal WAT and vastus explants from fasting mice (exposed to STD or HFD diets during 2 or 6 weeeks) were incubated ex-vivo under 95% O2 + 5% CO2 conditions at 37°C for 15 min, in free in DMEM free of serum, glucose and sodium pyruvate (Thermo Fisher Scientific Waltham, MA, USA). Insulin (100 nM, Actrapid, Novo Nordisk A/S, Bagsværd, Denmark) was added for additional 15 min and 0.1mM of the fluorescent D-glucose analogue 2-[N(7nitrobenz-2-oxa-1, 3-diazol-4-yl)amino]-2-deoxy-glucose (2-NBDG, Sigma-Aldrich, St. Louis, MO, USA) was added for 30 min more. Free 2-NBDG was washed out 3 times with cold PBS, tissues were lysed and intracellular 2-NBDG fluorescence (excitation 485 nm, emission 535 nm) was measured (VICTORX4, PerkinElmer, Waltham, MA, USA). Glucose uptake rates were calculated after subtracting the tissue background signal (negative control, without 2-NBDG) and normalized to tissue weights.

Reverse transcription–quantitative polymerase chain reaction (RT-qPCR)

All products and equipment used were from Thermo Fisher Scientific (Waltham, MA, USA). Tissues (epididymal WAT, vastus or liver) collected from fasting mice exposed to the diets (STD or HFD) during 2 or 6 weeeks were processed with Trizol to extract total RNA. Equal amounts of RNA were transcribed to cDNA with High Capacity cDNA RT Kit, and 10ng of cDNAs were amplified in a 7500 qPCR thermocycler. TaqMan gene expression assays were used to quantify AQP9 (Mm00508097_m1), GLUT2 (Mm00446229_m1), HSL (Mm00495359_m1), MCP-1 (Mm00441242_m1), PCK-1 (Mm01247058_m1), TNFα (Mm00443258_m1) and β-actin (Mm01205647_g1). To quantify the non-excised ILK sequence between exons within the floxed area number 6 and 7 in CRE-LOX mice, the following tandem primers were specially designed to be used with SYBR Green Master Mix: GGGCTCTTGTGAGCTTCTGT and GAGTGGTCCCCTTCCAGAAT [8, 11]. SYBR Green Master Mix and primers tandems were used to quantify GLUT4 (ATGGCTGTCGCTGGTTTCTC and TAAGGACCCATAGCATCCGC) and β-actin (GACGGCCAGGTCATCACTAT and CTTCTGCATCCTGTCAGCAA). Amplification values were normalized to endogenous β-actin ones and the relative quantification normalized of gene expression 2^−ΔΔCT method was used.

Protein extraction and immunoblot analysis

Tissues (epididymal WAT, vastus or liver) collected from fasting mice exposed to the diets (STD or HFD) during 2 or 6 weeks were homogenized in lysis buffer (10 mM Tris-HCl, pH 7.6; 1% Triton X-100; 1 mM EDTA; 0.1% sodium deoxycholate) supplemented with protease and phosphatase inhibitors (Complete and PhosSTOP, Roche, Basel, Switzerland). Protein concentrations were determined by DC-Protein Assay (Bio-Rad, Hercules, CA, USA). Equal amounts were separated on SDS-polyacrylamide gels and transferred to 0.2µm- PVDF membranes (Bio-Rad, Hercules, CA, USA). Membranes were blocked, incubated with primary antibodies against GLUT4 (Santa Cruz, Dallas, TX, USA), ILK (Cell Signaling Technology, Inc., Danvers, MA, USA), Actin or GAPDH (Sigma-Aldrich, St. Louis, MO, USA), and secondary antibodies (Merck-

Millipore, Billerica, MA, USA or Dako, Glostrup, Denmark) afterwards. Immunoblots were detected by chemiluminescence (Pierce ECL Western Blotting Substrate, Thermo Fisher Scientific Waltham, MA, USA) and imaged with ImageQuant LAS 500 System (General Electric Healthcare, Little Chalfont, Buckinghamshire, United Kingdom). Densitometries were measured using ImageJ software (NIH). Actin and GAPDH proteins were used as endogenous control.

Statistics

The data are represented as the means ± SEMs of a variable number of experiments detailed in the figure legends. Student's t test was used for 2 groups and 1- or 2-way analysis of variance was used for >2 groups (ANOVA) followed by Bonferroni's post hoc tests. Differences in mean values were considered statistically significant at a probability level of less than 5% ($p < 0.05$). Power of the study was 80-85%, depending on the number of animals per experiment, with a confidence level of 95%.

Results

In vivo transgenical ILK depletion exacerbates the disruption of glycaemic and lipidic patterns under a short-term HFD challenge

In our previous works we nominated "conditional knock-down" ILK mice (cKD-ILK) to the adult animals where ILK expression levels of mRNA and protein are partially depleted in adipose and skeletal muscle between other tissues, compared to their control littermates with the same transgenic background, but without ILK depletion (CT) [9, 12].

In order to study the role of ILK at the beginning of insulin resistance-related glycemic imbalance based in a HFD model, we challenged cKD-ILK or CT for 2 and 6 weeks with HFD or the matching STD (standard diet with low fat and sucrose). Diet composition, food and caloric intakes per 24 h of each group are shown in Table 1. No differences were observed between CT and cKD-ILK intakes subjected to the same diet. Both CT and cKD-ILK food intakes were slightly shorter under HFD compared to STD, although calories ingestion was higher in HFD-fed mice due to its caloric density. The reduced HFD ingestion is probably due to food adaptation, as observed in others similar models [15-18]. Biochemical determinations in blood, weight gains and other metabolic values where followed in fasting conditions along the 6 weeks of HFD in the same animals at the time points 0, 2 and 6 weeks. Fig. 1A show that basal fasting glycaemia in cKD-ILK was significantly higher than CT at time 0 of HFD, in accordance with our previous work [9]. During the HFD challenge, glycaemia progressively increased in both groups the 2nd week and steadily maintained high the 6th week of HFD. The highest values were reach by HFD-fed cKD-ILK as early as the 2nd week, surpassing the values of CT counterparts at the same time. Fig. 1B shows a similar pattern of fasting insulinemia from HFD-fed mice, being cKD-ILK those reaching the highest insulinemia at the 2nd week, although basal values between cKD-ILK and CT were not different at time 0 [9]. Glycaemia and insulinemia values from the same animal can be combined together to represent a reliable approximation of insulin resistance grade by using HOMA-IR indexes. These are the ratio changes (means + SEM) of HOMA-IR compared to CT 0 weeks from a total of n=12 of each group: CT 0w=1.08 + 0.12; CT 2w= 3.40 + 0.29*; CT 6w= 4.55 + 0.29*; cKD-ILK 0w= 1.47 + 0.12*,#; cKD-ILK 2w= 5.59 + 0.61*,#; cKD-ILK 6w= 5.43 + 0.42*,# , where *= $P<0.05$ vs 0w; #=$P<0.05$ vs CT at the same time point. These data confirmed the faster insulin sensitivity loss in cKD-ILK during the short-term exposure to HFD. To understand better the fragile glycemic profile along the 6 weeks, other group of cKD-ILK and CT were challenged to HFD for the same periods of time and subjected to intraperitoneal glucose tolerance tests (GTT). Fig. 1C shows the area under the glycemic curves resulted from the GTT (AUC). The 2nd week of HFD, AUC were progressively increased in both CT and cKD-ILK and maintained high the 6th week. cKD-ILK exhibited the greatest degree of glucose intolerance the 2nd week surpassing CT counterparts values. Because the glycaemic imbalance observed during HFD may be due to increased gluconeogenesis in the liver [3, 4], cKD-ILK and CT mice challenged to HFD were subjected to an intraperitoneal pyruvate tolerance test (PTT), a precursor of

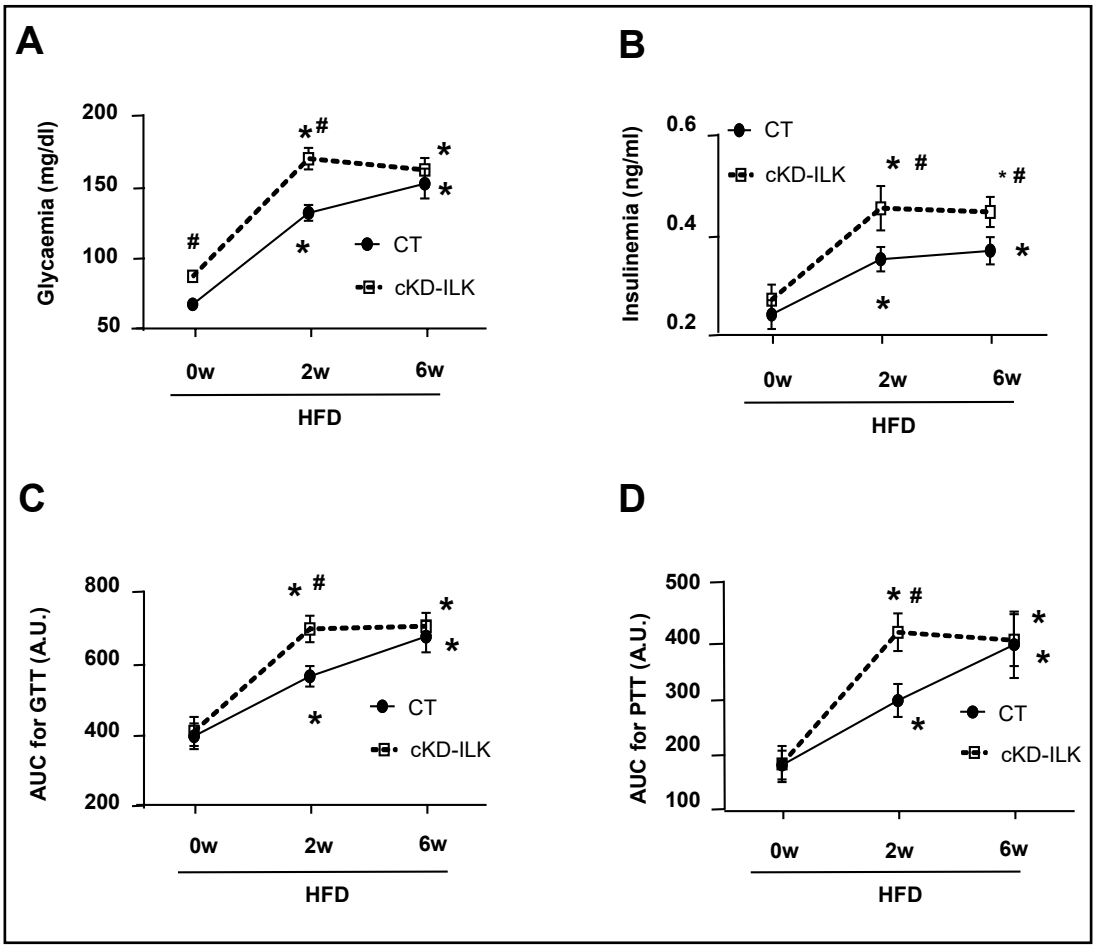

Fig. 1. Systemic glucose homeostasis and insulin sensitivity in CT and cKD-ILK along 6 weeks of HFD challenge. Blood glucose (A) and insulin (B) levels determined after fasting conditions from CT and cKD-ILK with HFD at time points 0, 2 and 6 weeks (w). Blood glucose levels during intraperitoneal glucose tolerance test (GTT) (C), and pyruvate tolerance test (PTT) (D), expressed as the areas under the curve (AUC). N=12 per group. All data are represented as means ± SEMs. *= P<0.05 vs 0w; #=P<0.05 vs CT at the same time point.

hepatic gluconeogenesis. Fig. 1D shows the glycemic values represented as AUC from the PTT, which progressively increased in both CT and cKD-ILK and maintained high the 6th week. cKD-ILK exhibited the greatest degree of gluconeogenesis the 2nd week, surpassing CT counterparts.

During HFD challenge in rodent models, body weight and circulating lipid determinants are changed [8, 15-18]. Fig. 2A shows the body weight gains of cKD-ILK and CT along the HFD implementation (0, 2 and 6 weeks). At the beginning of the diet challenge (time 0 weeks of HFD), no differences were observed between cKD-ILK and CT, but the values progressively increased in both groups the 2nd week and steadily maintained high the 6th week of HFD. cKD-ILK reached the highest values as early as the 2nd week surpassing the values of CT counterparts at the same time. Fig. 2B show unaltered plasmatic triglycerides values along the HFD challenge in both cKDILK and CT. Fig. 2C and 2D show that only in CT mice, the plasmatic total cholesterol and HDL levels were significantly increased the 2nd week to drop back to basal levels the 6th week of HFD. In cKD-ILK, values remained unaltered through the 6 weeks. Because the lipid metabolites seems to be altered in cKD-ILK challenged with HFD, we determined the two circulating lipolysis products glycerol and free fatty acids (FFA). As shown in Fig. 2E, blood glycerol levels significantly increase in both CT and cKD-ILK the 2nd

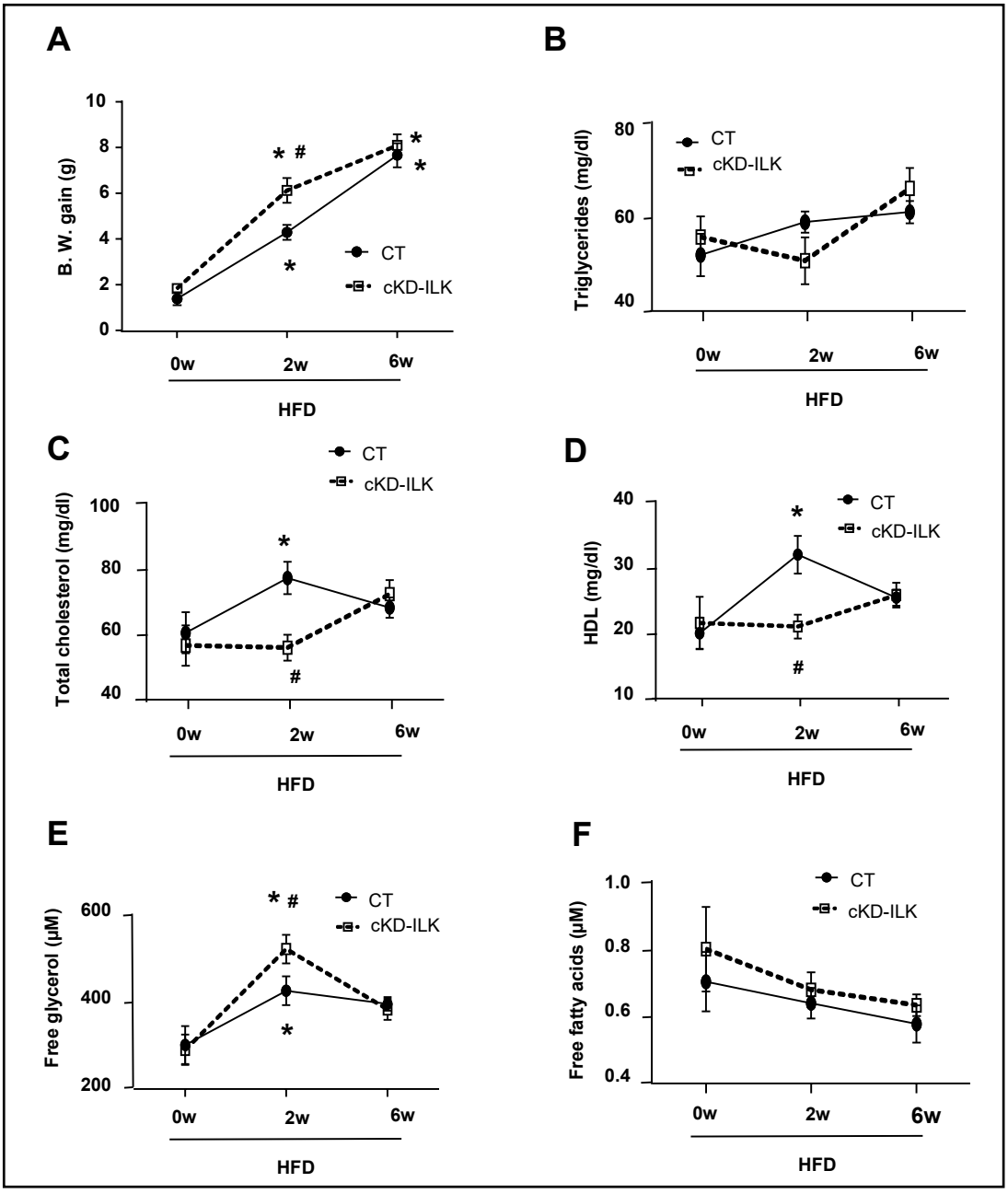

Fig. 2. Body weight gain and blood lipidic profiles in CT and cKD-ILK along 6 weeks of HFD challenge. Body weight (B.W.) gain (A) and blood levels of triglycerides (B), total cholesterol (C), HDL cholesterol (D), free glycerol (E) and free fatty acids (F) levels determined after fasting conditions from CT and cKD-ILK with HFD at time points 0, 2 and 6 weeks (w). N=12 per group. All data are represented as means ± SEMs. *= P<0.05 vs 0w; #=P<0.05 vs CT at the same time point.

week to drop to lower levels the 6th week, but still higher than basal values. In all this time line, cKD-ILK exhibited the greatest circulating glycerol value the 2nd week, surpassing any other counterparts values. However, Fig. 2F shows unaltered blood FFA levels in both CT and cKD-ILK mice challenged with HFD at any time.

ILK expression is reduced in peripheral insulin-sensitive tissues at the early implementation of HFD, leading to glucose uptake deterioration in the tissues

The biochemical parameters shown in the previous figures suggested that transgenic ILK downregulation relates to an early glycemic imbalance. Taking in consideration that we already demonstrated that cKD-ILK mice model featured basal hyperglycemia [9] and related to the partially depleted insulin-sensitive tisular ILK content (mRNA and protein), we further study the connection between ILK content and HFD challenge.

Thus, we subjected to HFD or STD for either 2 or 6 weeks to new groups of CT animals, where ILK is not transgenically depleted before the HFD challenge, and we determined the expression of ILK levels (either mRNA and/or protein contents) in some of their metabolic relevant tissues.

Fig. 3 shows that HFD dramatically downregulated the mRNA expression levels of ILK in CT compared to STD-fed CT, as soon as the 2nd week and as the same extent the 6th week, in the following tissues: epididymal depot of WAT (Fig. 3A), skeletal muscle (vastus, Fig. 3C) and liver (Fig. 3D). Fig. 3B, 3C, and 3E show that tisular ILK protein levels correlates with the mRNA downregulation in HFD-treated CT compared with STD-treated counterparts the 6th week. It is important to notice that the downregulation of WAT and skeletal muscle tisular expression of ILK in HFD-fed CT were at the same extent (around 50% decrease) to the already shown in basal cKD-ILK tissues [9].

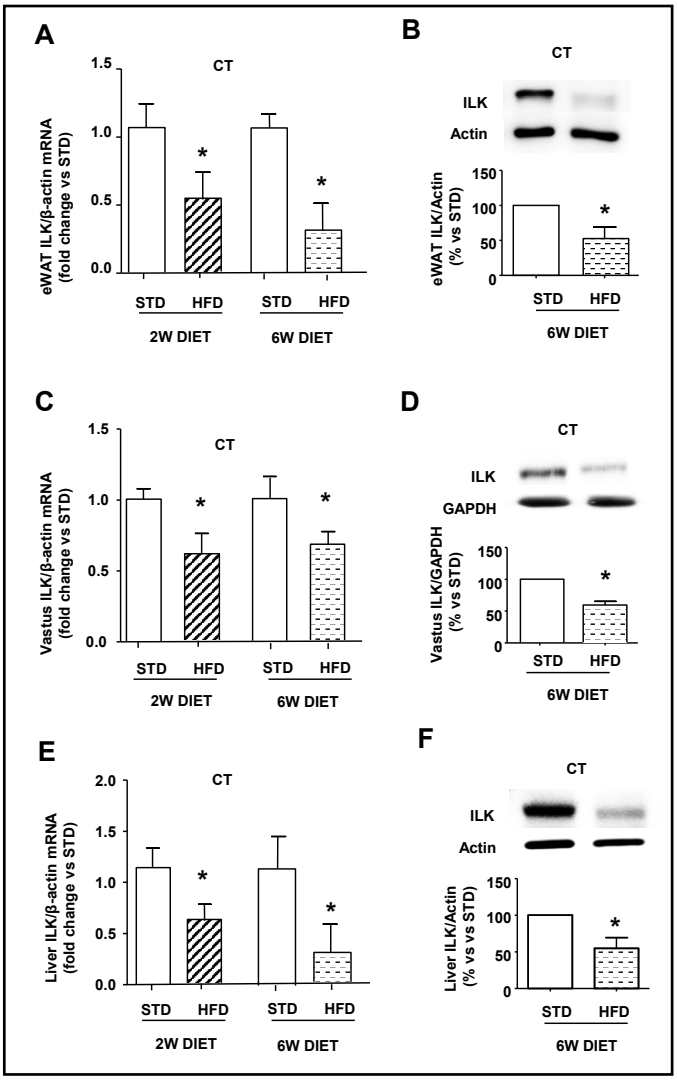

Fig. 3. ILK expression in adipose, skeletal muscle and hepatic tissues from CT during short-term STD or HFD challenges. Fresh isolated epididymal white adipose tissue (eWAT), vastus and liver explants were extracted from CT fed with either STD or HFD for 2 or 6 weeks (w). Animals were maintained in fasting conditions before to extract the tissues and proceed to the determinations. ILK mRNA expression levels fold changes, analyzed by RT-qPCR and normalized to β-actin as endogenous control, in eWAT (A), vastus (C) and liver (E) from CT fed with either STD or HFD for 2 or 6 weeks (w). Representative immunoblots and densitometric analysis of ILK protein levels normalized to Actin or GAPDH as endogenous control from eWAT (B), vastus (C) and liver (E) of CT fed with either STD or HFD for 6w. ILK expression transgenically downregulated in basal cKD-ILK tissues has been previously shown (Hatem-Vaquero M et al. J Endocrinol. 2017 Aug;234(2):115-128). N=12 per group. All data are represented as means ± SEMs. *= P<0.05 vs STD at the same time point.

Because we previously demonstrated that transgenic ILK downregulation in basal cKD-ILK relates intimately to the transcriptional downregulation of GLUT4 expression in WAT and skeletal muscle and its subsequent lack of functionality [9], we wonder whether early ILK downregulation due to the HFD implementation was related with the glucose uptake deterioration in the tissue. Thus, we determined the expression of GLUT4 in the same CT studied in the previous figure. Fig. 4 shows GLUT4 expression pattern similar to ILK, where HFD dramatically downregulates the mRNA expression levels of GLUT4 compared to STD, as soon as the 2nd week, in CT epididymal WAT (Fig. 4A) and vastus (Fig. 4D). GLUT4 protein levels correlates with the mRNA downregulation in HFD-treated CT the 6th week (Fig. 4B and 4E). To link the deteriorated glucose homeostasis with the downregulated ILK expression due to the HFD implementation, we studied the functional activity of GLUT4 in WAT and

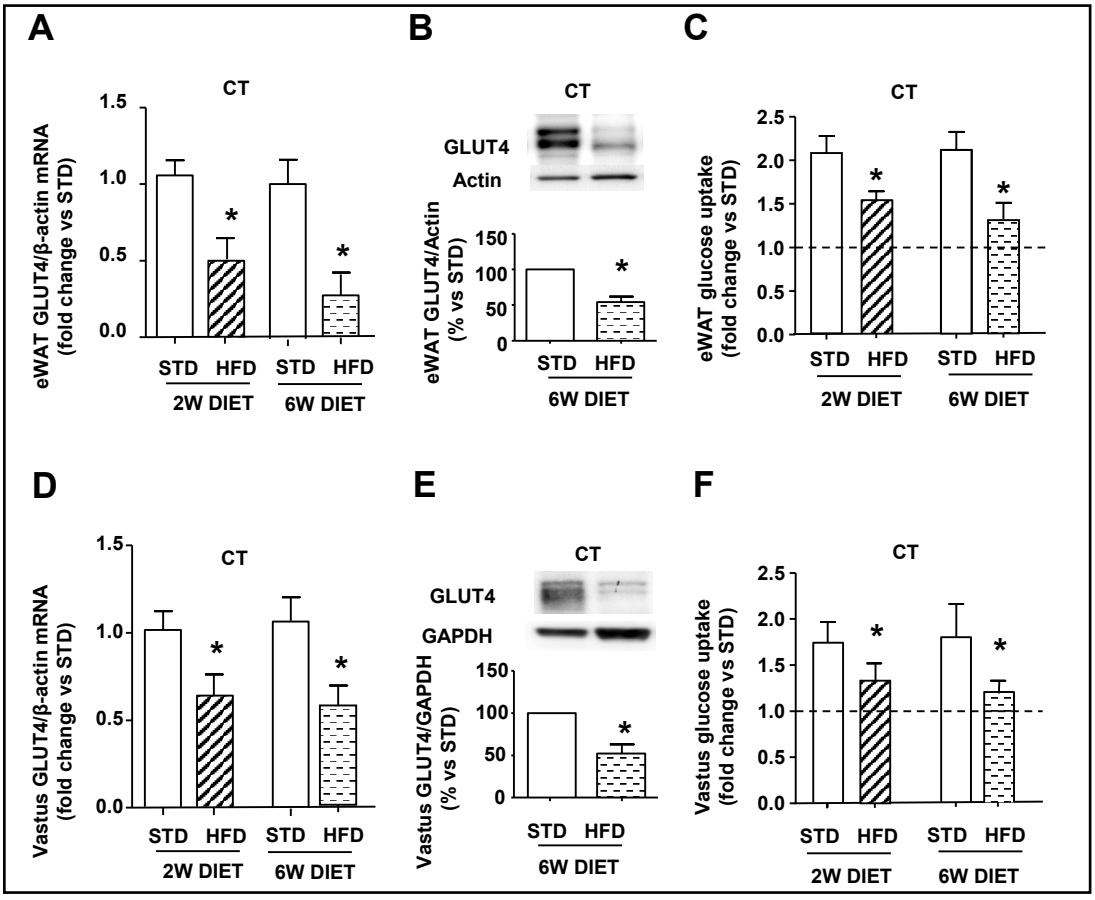

Fig. 4. Glucose transport profile in adipose and skeletal muscle tissues from CT during short-term STD or HFD challenges: GLUT4 expression and insulin-stimulated glucose uptake capacity. Fresh isolated epididymal white adipose tissue (eWAT) and vastus explants were extracted from CT fed with either STD or HFD for 2 or 6 weeks (w). Animals were maintained in fasting conditions before to extract the tissues and proceed to the determinations. GLUT4 mRNA expression levels fold changes, analyzed by RT-qPCR and normalized to β-actin as endogenous control, in eWAT (A) and vastus (D) from CT. Downregulated transcriptional GLUT4 downregulation was demonstrated previously in basal cKD-ILK tissues (Hatem-Vaquero M et al. J Endocrinol. 2017 Aug;234(2):115-128). Representative immunoblots and densitometric analysis of GLUT4 protein levels normalized to Actin or GAPDH as endogenous control from eWAT (B) and vastus (E) of CT fed with either STD or HFD for 6w. Other explants were incubated ex vivo with insulin (100 nM) for 15 min and the fluorescent deoxyglucose analog 2-NBDG (0.1 mM) was added for additional 30 min. The intracellular 2-NBDG fluorescence fold change was determined. Dashed line represents the STD-fed CT basal fluorescence from explants without insulin stimulation. N=12 per group. All data are represented as means ± SEMs. *= P<0.05 vs STD at the same time point.

skeletal muscle from CT challenged to either STD or HFD for 2 or 6 weeks. Tissues explants were manipulated ex-vivo, with or without the canonical stimulation of GLUT4-dependent glucose uptake by insulin. Fig. 4C and 4F show lower glucose uptake capabilities of WAT and vastus under insulin stimulation in HFD compared to STD at any time of diets exposure, consequent to the GLUT4 downregulations observed in HFD-treated CT and cKD-ILK [9].

Transgenic and/or HFD-mediated ILK reduction in WAT co-relates with the imbalanced markers expression of WAT lipolysis and inflammation, hepatic gluconeogenesis and related metabolites transporters

In Fig. 2E we already saw that circulating glycerol is temporary increased in cKD-ILK under HFD challenge. Thus, we studied whether the lipolysis pattern in the adipose tissue is altered when ILK is downregulated, either when ILK is depleted by transgenesis and/or during HFD-challenge. Fig. 5A and 5B shows the expression levels of the lipolysis marker hormone-sensitive lipase (HSL) in WAT from CT and cKD-ILK subjected with HFD or STD for either 2 or 6 weeks. Fig. 5A shows the expression levels of the lipolysis marker hormone-sensitive lipase (HSL) in WAT from CT and cKD-ILK subjected with HFD or STD for 2 weeks. cKD-ILK exhibited the greatest degree of HSL expression, surpassing CT counterparts values. Fig. 5B shows the expression levels of HSL in WAT from CT and cKD-ILK subjected with

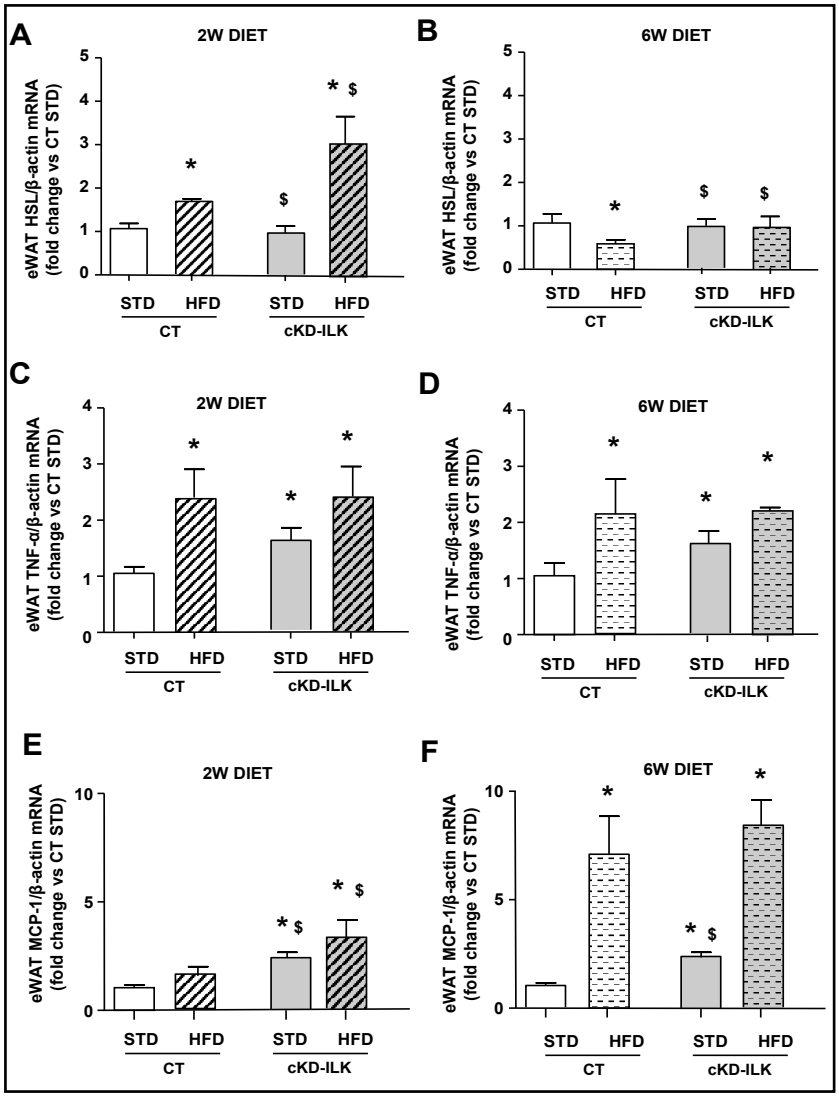

Fig. 5. Adipose expression of lipolysis and inflammatory markers from CT and cKD-ILK during short-term STD or HFD challenges. Fresh isolated epididymal white adipose tissue (eWAT) explants were extracted from CT and cKD-ILK fed with either STD or HFD for 2 or 6 weeks (w). Animals were maintained in fasting conditions before to extract the tissues and proceed to the determinations. Lipase HSL (A, B) and pro-inflamatory adipokines TNFα (C, D) and MCP-1 (E, F) mRNA expression levels fold changes, analyzed by RT-qPCR and normalized to β-actin as endogenous control. N=12 per group. All data are represented as means ± SEMs. *= P<0.05 vs CT STD, $=P<0.05 vs CT HFD.

HFD or STD for 6 weeks. In this time point, CT fed with HFD reduced their HSL expression to a significant lower level than CT fed with STD. Although HFD-fed cKD-ILK levels where not different to STD-fed cKD-ILK, they remained significantly higher than HFD-fed CT. The temporary increase and drop of HSL expression correlates with the pattern of circulating glycerol shown in Fig. 2.

Because the increase of pro-inflammatory adipokines expression in WAT is one of the well-known events that occurs during HFD-mediated adipocyte dysfunction in animal models [15-18], we studied mRNA levels of TNFα and MCP-1 in the same animal groups. Fig. 5C and 5D show that, under basal conditions, STD-fed cKD-ILK exhibited increased expression levels of TNFα compared to STD-fed CT, and once HFD was challenged for 2 (Fig. 5C) or 6 weeks (Fig. 5D), CT and cKD-ILK animals increased their WAT expression at the same extent as the basal STD-fed cKD-ILK. Similarly, Fig. 5E and 5F show that STD-fed cKD-ILK exhibited a basal increase in the expression of MCP-1 cytokine. The 2nd week of HFD did not change the MCP-1 expression pattern in CT compared to basal, but increased in HFD-fed cKD-ILK surpassing the HFD-fed CT values (Fig. 5E). The maximal peak of MCP-1 expression was reached the 6th week of HFD in both CT and cKD-ILK (Fig. 5F).

As mentioned previously, glucose homeostasis is coordinated between peripheral tissues glucose uptakes and the endogenous glucose production by the liver [3, 4]. The increased stress to pyruvate in HFD-fed cKD-ILK shown in Fig. 1 together with the reduced expression of ILK in the liver shown in Fig. 3 implies a relation between hepatic ILK and gluconeogenesis during HFD challenge. The expression levels of the hepatic glycerol-independent gluconeogenesis limiting enzyme phosphoenolpyruvate carboxykinase 1 (PCK-1) are shown in the 2 weeks (Fig. 6A) and 6 weeks (Fig. 6B) diets challenge. During HFD, the expression was higher in both genotypes than STD-fed animals. 2 weeks HFD-fed cKD-ILK exhibited the greatest PCK-1 expression values (Fig. 6A). This peak of expression was reached by CT and cKD-ILK groups the 6th week, without differences between them (Fig. 6B). We further asked whether hepatic transporters for glucose and glycerol were changing their expression pattern by hepatic ILK downregulation shown in Fig. 3 and its implication in the imbalanced glucose and glycerol values observed in the blood of HFD-challenged mice, already shown in Fig. 1 and Fig. 2.

The main hepatic glycerol transporter AQP9 increase its expression after 2 weeks (Fig. 6C) and 6 weeks (Fig. 6D) of HFD, following a similar pattern of expression as PCK-1 and in accordance to the circulating glycerol increase shown in Fig. 1.

Under basal conditions during the 2 or 6 weeks of diet challenges, STD-fed cKD-ILK exhibited increased expression levels of the main hepatic glucose transporter GLUT2 (Fig. 6E and 6F). CT and cKD-ILK challenged for 2 weeks with HFD increased their hepatic GLUT2 expression at the same extent as the basal STD-fed cKD-ILK (Fig. 6E). The 6th week of HFD challenge (Fig. 6F), cKD-ILK livers reached the highest peak of GLUT2 expression, surpassing the HFD-fed CT.

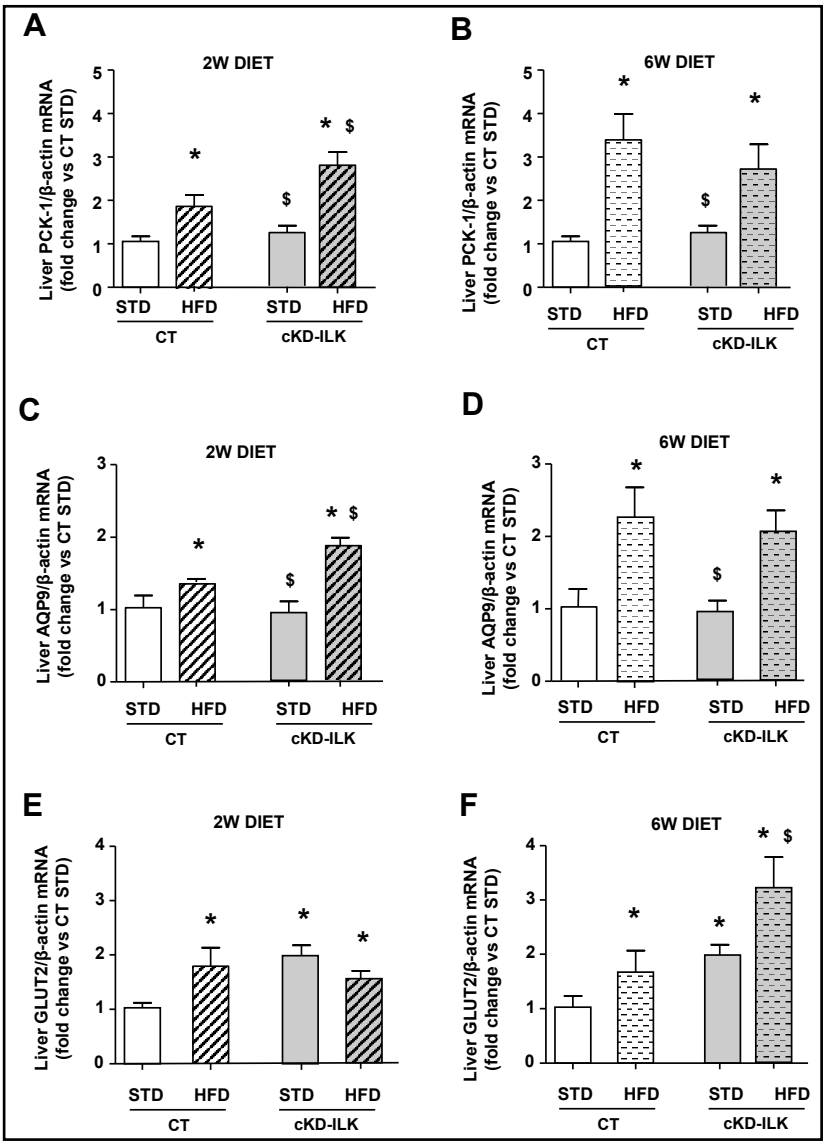

Fig. 6. Hepatic expression of gluconeogenesis marker and transmembrane transporters from CT and cKD-ILK during short-term STD or HFD challenges. Fresh isolated liver explants were extracted from CT and cKD-ILK fed with either STD or HFD for 2 or 6 weeks (w). Animals were maintained in fasting conditions before to extract the tissues and proceed to the determinations. Hepatic gluconeogenesis marker PCK-1 (A, B) and metabolites transporters AQP9 (C, D) and GLUT2 (E, F) mRNA expression levels fold changes, analyzed by RT-qPCR and normalized to β-actin as endogenous control. N=12 per group. All data are represented as means ± SEMs. *= P<0.05 vs CT STD, $=P<0.05 vs CT HFD.

Discussion

We demonstrated that transgenic or HFD-based ILK downregulation in the tissues relates with insulin resistance initiation during the early stages of a HFD-based model. Short term HFD models allow to study in few weeks the early stages of insulin impairment in relevant metabolic organs, which mimics a "pre-diabetes" state, whereas longer diet periods are devoted to study the clear "clinical" induction of obesity and diabetes [8, 15-18]. In cKD-ILK the ILK expression is blunted by transgenesis in insulin-sensitive tissues, under basal STD conditions and before to any HFD challenge [8]. Interestingly, the ILK downregulation itself in these animals is directly co-related with increased expression of pro-inflammatory WAT cytokines TNFα and MCP-1, decreased GLUT4 presence and increase hepatic GLUT2. Furthermore, at this basal point we may dissociate the effect of ILK-mediated changes in metabolism from the "preliminary" obesity state, because STD-fed cKD-ILK have those and other metabolic-related parameters imbalanced but are not accompanied by body weight changes [9]. Although we and others have shown that ILK deletion in other tissues may trigger anti-inflammatory effects [19-22] and considering that cytokines are in turn ILK expression modulators [23, 24], our results suggest that ILK loss is able to modulate the

expression of pro-inflammatory cytokines in metabolic-relevant tissues in accordance with other studies [25]. Moreover, the increased WAT cytokines may deregulate GLUT4 [26-29] and it is possible that ILK-dependent WAT-originated cytokines downregulates GLUT4. In any case, our results are not conclusive to assure whether ILK downregulation is the cause or the consequence of the pro-inflammatory state. Once the HFD is implemented, those pathological parameters are remarkably exacerbated in cKD-ILK when compared to the rest of counterparts, reaching maximum responses at very early stages, the 2nd week at the most of the cases. The imbalanced expressions of GLUT4 and GLUT2 are exacerbated and extended to the hepatic glycerol transporter AQP9 upregulation in HFD-fed cKD-ILK. This is probably related with the striking decrease of glucose disposal capability in WAT and muscle of HFD-stimulated cKD-ILK, the consequent hyperglycemia exacerbation, as well as further increase of body weight, WAT pro-inflammation and hepatic gluconeogenesis.

Because misbalanced metabolism implicates several tissues and conditions, the obesity or its establishment might be the origin but also the consequence of insulin resistance [30]. Although we think that ILK transgenic depletion can be dissociated from changes in body weight under STD conditions [9], the HFD-fed cKD-ILK rapidly increased their body weight, suggesting that ILK may relate with the development of obesity.

Other works with specific and non-inducible deletions of skeletal or hepatic ILK, basally or under HFD challenge, showed different insulin sensitive behaviors [10, 31-33] in contrast to our aggravated model. Without regards on the transgenic model used, our CT animals (where no transgenic ILK downregulation occurs at the initiation of the experiment) reached the dramatic downregulation of ILK expression in insulin-sensitive tissues as early as 2 weeks of HFD implementation. This is a very important highlight from our work: the ILK downregulation in such an early stage during the implementation or a HFD model may be a precise indicative of the original impairment of the modulation of metabolites.

The blood lipid profile in HFD animal models vary depending of several factors such as the animal genetic background, the percentage and nature of the fat or sugars used in the diet, the specific length of the HFD challenge or the fasting conditions when the animals were tested [8, 15-18, 34]. In our case, blood triglyceride was not different between animal groups. A temporary increase in total cholesterol and HDL levels in HFD-fed CT, but not in cKD-ILK counterparts, may be associated to a great flow of cholesterol adaptation [35] that disappeared the 6th week, and probably the adaptive mechanism was early blunted in cKD-ILK because an original ILK-based impairment.

Increased WAT lipolysis, quantified by circulating glycerol or HSL expression, is uncontrolled during chronic metabolic diseases [2, 35-37]. We observed early but apparently temporal increases of HSL expression and circulating glycerol. HFD-fed cKD-ILK reached the maximum of this lipolysis-like effect, and it can be understood as an autocrine effect of the increased WAT-originated cytokines [38-40] and/or the blocked mediation of the ILK-dependent downstream substrate AKT [2, 41]. Circulating FFA levels were not modified in our model, as previously observed in others´ short-term HFD models under fasting conditions [42, 43]. Some hypothesis to explain this point to the lack of "unrestrained" lipolysis in such a short-term HFD. Moreover, and considering the necessities of the fasted organism and the nutrient fluxes cross-talk between different organs, FFAs may substantially re-esterify into the adipocyte, or even be satisfactorily transported, up-taken and oxidized by other tissues [2, 3, 15-18, 34, 42, 43].

Activated hepatic gluconeogenesis is another source of hyperglycemia, where the substrate could be the increased plasmatic glycerol and/or other glycerol-independent gluconeogenesis catalyzed by overexpressed PCK-1 [4]. In our model, ILK downregulation inversely correlated with increased hepatic gluconeogenesis, in accordance with others´ hepatocyte-specific ILK knockout mice [31]. The hepatic expression of ILK was also downregulated in HFD-fed CT, in accordance with previous reports [33]. ILK-depletion (transgenic or HFD-induced) did not change liver weight (data not shown), in contraposition to other ILK-depleted model [32]. We hypothesize that ILK loss increases the circulating glycerol and inversely modulates hepatic PCK-1 expression. It is probable that ILK-dependent

hepatic AKT downregulation [41] is not able to blockade FOXO1-dependent PCK-1 promoter activity [44, 45]. Increased gluconeogenesis in our model, and in accordance with others' works, demanded for increased metabolites transport [46] as hepatic AQP9 [47, 48] and GLUT2 [6]. The unbalanced expression of the transmembrane transporters studied in this work (GLUT4, GLUT2 and AQP9) have been extensively observed in insulin-resistant and obese subjects and animal models [5, 6, 7, 47-53]. We [9-14] and indirectly others [11] demonstrated ILK-mediated transcriptional regulation of GLUT4 and AQP2, and here we observed that ILK downregulation during the HFD challenge converge with the unbalanced expression of those metabolite transporters, and interestingly opposite expression profiles of GLUT4 versus GLUT2 and AQP9 in the same animals are followed by the same ILK downregulation.

Conclusion

Considering all this, ILK presence loss might be a transcriptional master key of metabolites transporters and other inflammatory and metabolic markers. We conclude that ILK expression in peripheral tissues is an important predictive value during the early progression of insulin resistance and it may contribute in the pathogenesis of metabolic disorders.

Acknowledgements

This work was supported by co-founded grants from Instituto de Salud Carlos III (ISCIII), Comunidad de Madrid (NovelRen) and FEDER funds [grants PI14/01939, PI14/02075, PI17/01513, PI17/00625, S2017/BMD-3751], the FEDER and ISCIII RETIC REDinREN programs [grants RD12/0021/0006 and RD16/0009/0018], Instituto Ramon y Cajal de Investigación Sanitária (IRYCIS) [grant 3.07] and Fundación Renal Iñigo Álvarez de Toledo (FRIAT). Animal experiments have been approved by the Institutional Animal Care and Use Committees from Universidad de Alcalá and Comunidad de Madrid (PROEX 230/16), in agreement with the guidelines established by the European Community Council Directives (2010/63/EU).

Author contributions: SDF, MRP, DRP conceived the study. SDF designed the experimental plan and performed experiments. MHV, MG, DGA, SC and LB performed and analyzed experiments and contributed to the interpretation of the data. SDF, MRP wrote and edited the manuscript. MHV, DRP and LC revised critically the intellectual content of the project. All authors read edited the manuscript and approved the final submitted version.

Disclosure Statement

The authors have no conflicts of interest to declare.

References

1 Graham TE, Kahn BB: Tissue-specific alterations of glucose transport and molecular mechanisms of intertissue communication in obesity and type 2 diabetes. Horm Metab Res 2007;39:717-721.

2 Guilherme A, Virbasius JV, Puri V, Czech MP: Adipocyte dysfunctions linking obesity to insulin resistance and type 2 diabetes. Nat Rev Mol Cell Biol 2008;9:367-377.

3 Samuel VT, Liu ZX, Qu X, Elder BD, Bilz S, Befroy D, Romanelli AJ, Shulman GI: Mechanism of hepatic insulin resistance in non-alcoholic fatty liver disease. J Biol Chem 2004;279:32345-32353.

4 Sharabi K, Tavares CD, Rines AK, Puigserver P: Molecular pathophysiology of hepatic glucose production. Mol Aspects Med 2015;46:21-33.
5 Karnieli E, Armoni M: Transcriptional regulation of the insulin-responsive glucose transporter GLUT4 gene: from physiology to pathology. Am J Physiol Endocrinol Metab 2008;295:E38-E45.
6 Thorens B: GLUT2, glucose sensing and glucose homeostasis. Diabetologia 2015;58:221-232.
7 Lebeck J: Metabolic impact of the glycerol channels AQP7 and AQP9 in adipose tissue and liver. J Mol Endocrinol 2014;52:R165-R178.
8 Seferovic MD, Beamish CA, Mosser RE, Townsend SE, Pappan K, Poitout V, Aagaard KM, Gannon M: Increases in bioactive lipids accompany early metabolic changes associated with β-cell expansion in response to short-term high-fat diet. Am J Physiol Endocrinol Metab 2018;315:E1251-E1263.
9 Hatem-Vaquero M, Griera M, García-Jerez A, Luengo A, Álvarez J, Rubio JA, Calleros L, Rodríguez-Puyol D, Rodríguez-Puyol M, De Frutos S: Peripheral insulin resistance in ILK-depleted mice by reduction of GLUT4 expression. J Endocrinol 2017;234:115-128.
10 Kang L, Mokshagundam S, Reuter B, Lark DS, Sneddon CC, Hennayake C, Williams AS, Bracy DP, James FD, Pozzi A, Zent R, Wasserman DH: Integrin-Linked Kinase in Muscle Is Necessary for the Development of Insulin Resistance in Diet-Induced Obese Mice. Diabetes 2016;65:1590-1600.
11 Tang X, Guilherme A, Chakladar A, Powelka AM, Konda S, Virbasius JV, Nicoloro SM, Straubhaar J, Czech MP: An RNA interference-based screen identifies MAP4K4/NIK as a negative regulator of PPARgamma, adipogenesis, and insulin-responsive hexose transport. Proc Natl Acad Sci U S A 2006;103:2087-2092.
12 Cano-Peñalver JL, Griera M, Serrano I, Rodríguez-Puyol D, Dedhar S, de Frutos S, Rodríguez-Puyol M: Integrin-linked kinase regulates tubular aquaporin-2 content and intracellular location: a link between the extracellular matrix and water reabsorption. FASEB J 2014;28:3645-3659.
13 Mamuya FA, Cano-Peñalver JL, Li W, Rodriguez Puyol D, Rodriguez Puyol M, Brown D, de Frutos S, Lu HA: ILK and cytoskeletal architecture: an important determinant of AQP2 recycling and subsequent entry into the exocytotic pathway. Am J Physiol Renal Physiol 2016;311:F1346-F1357.
14 Hatem-Vaquero M, Griera M, Giermakowska W, Luengo A, Calleros L, Gonzalez Bosc LV, Rodríguez-Puyol D, Rodríguez-Puyol M, De Frutos S: Integrin linked kinase regulates the transcription of AQP2 by NFATC3. Biochim Biophys Acta Gene Regul Mech 2017;1860:922-935.
15 Park SY, Cho YR, Kim HJ, Higashimori T, Danton C, Lee MK, Dey A, Rothermel B, Kim YB, Kalinowski A, Russell KS, Kim JK: Unraveling the temporal pattern of diet-induced insulin resistance in individual organs and cardiac dysfunction in C57BL/6 mice. Diabetes 2005;54:3530–3540.
16 Winzell MS, Ahren B: The high-fat diet-fed mouse: a model for studying mechanisms and treatment of impaired glucose tolerance and type 2 diabetes. Diabetes 2004;53:S215–S219.
17 Masgrau A, Mishellany-Dutour A, Murakami H, Beaufrère AM, Walrand S, Giraudet C, Migné C, Gerbaix M, Metz L, Courteix D, Guillet C, Boirie Y: Time-course changes of muscle protein synthesis associated with obesity-induced lipotoxicity. J Physiol 2012;590:5199-5210.
18 Williams LM, Campbell FM, Drew JE, Koch C, Hoggard N, Rees WD, Kamolrat T, Thi Ngo H, Steffensen IL, Gray SR, Tups A: The development of diet-induced obesity and glucose intolerance in C57BL/6 mice on a high-fat diet consists of distinct phases. PLoS One 2014;9:e106159.
19 Alique M, Civantos E, Sanchez-Lopez E, Lavoz C, Rayego-Mateos S, Rodrigues-Díez R, García-Redondo AB, Egido J, Ortiz A, Rodríguez-Puyol D, Rodríguez-Puyol M, Ruiz-Ortega M: Integrin-linked kinase plays a key role in the regulation of angiotensin II-induced renal inflammation. Clin Sci (Lond) 2014;127:19-31.
20 Cano-Peñalver JL, Griera M, García-Jerez A, Hatem-Vaquero M, Ruiz-Torres MP, Rodríguez-Puyol D, Frutos S, Rodríguez-Puyol M: Renal Integrin-Linked Kinase Depletion Induces Kidney cGMP-Axis Upregulation: Consequences on Basal and Acutely Damaged Renal Function. Mol Med 2016;21:873-885.
21 de Frutos S, Luengo A, García-Jérez A, Hatem-Vaquero M, Griera M, O'Valle F, Rodríguez-Puyol M, Rodríguez-Puyol D, Calleros L: Chronic kidney disease induced by an adenine rich diet upregulates integrin linked kinase (ILK) and its depletion prevents the disease progression. Biochim Biophys Acta Mol Basis Dis 2019;1865:1284-1297.
22 Assi K, Patterson S, Dedhar S, Owen D, Levings M, Salh B: Role of epithelial integrin-linked kinase in promoting intestinal inflammation: effects on CCL2, fibronectin and the T cell repertoire. BMC Immunol 2011;12:42.

23 Friedrich EB, Sinha S, Li L, Dedhar S, Force T, Rosenzweig A, Gerszten RE: Role of integrin-linked kinase in leukocyte recruitment. J Biol Chem 2002;277:16371-16375.
24 Ruiz-Torres MP, Pérez-Rivero G, Rodríguez-Puyol M, Rodríguez-Puyol D, Díez-Marqués ML: The leukocyte-endothelial cell interactions are modulated by extracellular matrix proteins. Cell Physiol Biochem 2006;17:221-232.
25 Grzelkowska-Kowalczyk K, Tokarska J, Grabiec K, Gajewska M, Milewska M, Błaszczyk M: Tumor necrosis factor-α alters integrins and metalloprotease ADAM12 levels and signaling in differentiating myoblasts. Pol J Vet Sci 2016;19:253-259.
26 Sartipy P, Loskutoff DJ: Monocyte chemoattractant protein 1 in obesity and insulin resistance. Proc Natl Acad Sci U S A 2003;100:7265-7270.
27 Zhou W, Yang P, Liu L, Zheng S, Zeng Q, Liang H, Zhu Y, Zhang Z, Wang J, Yin B, Gong F, Wu Y, Li Z: Transmembrane tumor necrosis factor-alpha sensitizes adipocytes to insulin. Mol Cell Endocrinol 2015;406:78-86.
28 Ruan H, Miles PD, Ladd CM, Ross K, Golub TR, Olefsky JM, Lodish HF: Profiling gene transcription *in vivo* reveals adipose tissue as an immediate target of tumor necrosis factor-alpha: implications for insulin resistance. Diabetes 2002;51:3176-3188.
29 Nieto-Vazquez I, Fernández-Veledo S, Krämer DK, Vila-Bedmar R, Garcia-Guerra L, Lorenzo M: Insulin resistance associated to obesity: the link TNF-alpha. Arch Physiol Biochem 2008;114:183-194.
30 Czech MP: Insulin action and resistance in obesity and type 2 diabetes. Nat Med 2017;23:804-814.
31 Williams AS, Trefts E, Lantier L, Grueter CA, Bracy DP, James FD, Pozzi A, Zent R, Wasserman DH: Integrin-Linked Kinase Is Necessary for the Development of Diet-Induced Hepatic Insulin Resistance. Diabetes 2017;66:325-334.
32 Gkretsi V, Apte U, Mars WM, Bowen WC, Luo JH, Yang Y, Yu YP, Orr A, St-Arnaud R, Dedhar S, Kaestner KH, Wu C, Michalopoulos GK: Liver-specific ablation of integrin-linked kinase in mice results in abnormal histology, enhanced cell proliferation, and hepatomegaly. Hepatology 2008;48:1932-1941.
33 Trefts E, Hughey CC, Lantier L, Lark DS, Boyd KL, Pozzi A, Zent R, Wasserman DH: Energy Metabolism Couples Hepatocyte Integrin-linked Kinase to Liver Glucoregulation and the Postabsorptive Response of Mice in an Age-dependent Manner. Am J Physiol Endocrinol Metab 2019;316:E1118-E1135.
34 Montgomery MK, Hallahan NL, Brown SH, Liu M, Mitchell TW, Cooney GJ, Turner N: Mouse strain-dependent variation in obesity and glucose homeostasis in response to high-fat feeding. Diabetologia 2013;56:1129-1139.
35 Hayek T, Azrolan N, Verdery RB, Walsh A, Chajek-Shaul T, Agellon LB, Tall AR, Breslow JL: Hypertriglyceridemia and cholesteryl ester transfer protein interact to dramatically alter high density lipoprotein levels, particle sizes, and metabolism. Studies in transgenic mice. J Clin Invest 1993;92:1143-1152.
36 Ter Horst KW, van Galen KA, Gilijamse PW, Hartstra AV, de Groot PF, van der Valk FM, Ackermans MT, Nieuwdorp M, Romijn JA, Serlie MJ: Methods for quantifying adipose tissue insulin resistance in overweight/obese humans. Int J Obes (Lond) 2017;41:1288-1294.
37 Schweiger M, Schreiber R, Haemmerle G, Lass A, Fledelius C, Jacobsen P, Tornqvist H, Zechner R, Zimmermann R: Adipose triglyceride lipase and hormone-sensitive lipase are the major enzymes in adipose tissue triacylglycerol catabolism. J Biol Chem 2006;281:40236-40241.
38 Hube F, Hauner H: The role of TNF-alpha in human adipose tissue: prevention of weight gain at the expense of insulin resistance?. Horm Metab Res 1999;31:626-631.
39 Wellen KE, Hotamisligil GS: Obesity-induced inflammatory changes in adipose tissue. J Clin Invest 2003;112:1785-1788.
40 Sethi JK, Hotamisligil GS: The role of TNF alpha in adipocyte metabolism. Semin Cell Dev Biol 1999;10:19-29.
41 Troussard AA, Mawji NM, Ong C, Mui A, St -Arnaud R, Dedhar S: Conditional knock-out of integrin-linked kinase demonstrates an essential role in protein kinase B/Akt activation. J Biol Chem 2003;278:22374-22378.
42 Wiedemann MS, Wueest S, Grob A, Item F, Schoenle EJ, Konrad D: Short-term HFD does not alter lipolytic function of adipocytes. Adipocyte 2014;3:115-120.
43 Jin ES, Beddow SA, Malloy CR, Samuel VT: Hepatic glucose production pathways after three days of a high-fat diet. Metabolism 2013;62:152-162.

44 Cheng Z, White MF: Targeting Forkhead box O1 from the concept to metabolic diseases: lessons from mouse models. Antioxid Redox Signal 2011;14:649-661.
45 Wang Q, Wang N, Dong M, Chen F, Li Z, Chen Y: GdCl3 reduces hyperglycaemia through Akt/FoxO1-induced suppression of hepatic gluconeogenesis in Type 2 diabetic mice. Clin Sci (Lond) 2014;127:91-100.
46 Klover PJ, Mooney RA: Hepatocytes: critical for glucose homeostasis. Int J Biochem Cell Biol 2004;36:753-758.
47 Rojek AM, Skowronski MT, Füchtbauer EM, Füchtbauer AC, Fenton RA, Agre P, Frøkiaer J, Nielsen S: Defective glycerol metabolism in aquaporin 9 (AQP9) knockout mice. Proc Natl Acad Sci U S A 2007;104:3609–3614.
48 Calamita G, Gena P, Ferri D, Rosito A, Rojek A, Nielsen S, Marinelli RA, Frühbeck G, Svelto M: Biophysical assessment of aquaporin-9 as principal facilitative pathway in mouse liver import of glucogenetic glycerol. Biol Cell 2012;104:342-351.
49 Minokoshi Y, Kahn CR, Kahn BB: Tissue-specific ablation of the GLUT4 glucose transporter or the insulin receptor challenges assumptions about insulin action and glucose homeostasis. J Biol Chem 2003;278:33609-33612.
50 Atkinson BJ, Griesel BA, King CD, Josey MA, Olson AL: Moderate GLUT4 overexpression improves insulin sensitivity and fasting triglyceridemia in high-fat diet-fed transgenic mice. Diabetes 2013;62:2249-2258.
51 Abel ED, Peroni O, Kim JK, Kim YB, Boss O, Hadro E, Minnemann T, Shulman GI, Kahn BB: Adipose-selective targeting of the GLUT4 gene impairs insulin action in muscle and liver. Nature 2001;409:729-733.
52 Zisman A, Peroni OD, Abel ED, Michael MD, Mauvais-Jarvis F, Lowell BB, Wojtaszewski JF, Hirshman MF, Virkamaki A, Goodyear LJ, Kahn CR, Kahn BB: Targeted disruption of the glucose transporter 4 selectively in muscle causes insulin resistance and glucose intolerance. Nat Med 2000;6:924-928.
53 Rodríguez A, Gena P, Méndez-Giménez L, Rosito A, Valentí V, Rotellar F, Sola I, Moncada R, Silva C, Svelto M, Salvador J, Calamita G, Frühbeck G: Reduced hepatic aquaporin-9 and glycerol permeability are related to insulin resistance in non-alcoholic fatty liver disease. Int J Obes (Lond) 2014;38:1213-1220.